*Desalination and Water Treatment*
www.deswater.com
doi: 10.5004/dwt.2022.28476

259 (2022) 45–53
May

# Desalination of seawater with pervaporation technology by using poly(vinyl alcohol)/chitosan-*g*-poly(*N*,*N*-dimethylacrylamide) membranes

Fatma Kurşun Baysak, Cemile Özcan*

*Department of Chemistry, Faculty of Art and Sciences, Kirklareli University, 39100 Kirklareli, Turkey, emails: cemilebal.ozcan@klu.edu.tr (C. Özcan), fatma.kursun@klu.edu.tr (F.K. Baysak)*

Received 1 September 2021; Accepted 6 April 2022

**ABSTRACT**

In our world, where the need for clean water is increasing, the importance of obtaining drinking and utility water by desalinating seawater is expanding. For this purpose, in this study, poly(vinyl alcohol)/(chitosan-*g*-poly(*N*,*N*-dimethylacrylamide)) (PVA/CS-*g*-PNDMAAm) membranes were used for seawater desalination through pervaporation technology. Firstly, CS-*g*-PNDMAAm copolymers were synthesized and then characterized by Fourier-transform infrared spectroscopy and thermogravimetric analysis. Afterward, PVA/CS-*g*-PNDMAAm membranes were prepared, and their surfaces were characterized by scanning electron microscopy–energy-dispersive X-ray analysis. The effects of the pH, CS-*g*-PNDMAAm percentage and, working temperature on the salt rejection and flux were investigated by separating Na/water mixtures with the pervaporation technique. In removing Na from Marmara Seawater using the pervaporation technique, the maximum salt rejection was 99.94. At the same time, the flux was 993.52 g $m^{-2}$ $h^{-1}$ under optimum conditions (pH: 8, *T*: 25°C, CS-*g*-PNDMAAm percentage: 25%).

*Keywords:* Desalination; Pervaporation; Chitosan; Poly(vinyl alcohol); *N*,*N*-dimethylacrylamide

## 1. Introduction

The shortage of clean water has become one of the most critical problems in the world with the rapid increase in global population and urbanization, climate change, and contamination of available freshwater resources [1–3]. The World Health Organization (WHO) estimates that 2.1 billion people are deprived of safe drinking water sources, and the World Water Council (WWC) estimates that 3.9 billion people around the world will live in areas with water scarcity by 2030 [4]. Desalination of seawater to obtain drinking water has aroused great interest in solving the water crisis worldwide. Desalination technology is generally using highly selective membrane technologies such as seawater reverse osmosis (SWRO) [5–8], membrane distillation [9–12] and pervaporation (PV) [1,3,13,14]. However, SWRO technology has disadvantages such as being able to process seawater with only 3% to 4% NaCl content by weight and high energy consumption; reverse osmosis (RO) technology has disadvantages such as process design limitations, high fouling propensity, low water recovery from seawater desalination (35%–55%) and high pressure (over 50 bar) [15–18]. PV technology has been used for desalination in recent years and dehydration of azeotropic and near boiling point mixtures. Xie et al. [19] also reported a high salt rejection (>99.5%) and water flux (6.93 kg $m^2$ $h^{-1}$) using a sol–gel derived poly(vinyl alcohol)/maleic acid/silica hybrid membrane by pervaporation. Gazagnes et al. [20] declared the seawater desalination by pervaporation with a hydrophobic zirconia membrane, which played a highest salt rejection (>95%) and flux (1.6 kg $m^2$ $h^{-1}$). Nigiz [21] expressed the highest rejection of 99.95% with a flux of 3.46 kg $m^2$ $h^{-1}$ was achieved at 40°C by using 1 wt.% of GO filled alginate membrane to desalination of seawater by pervaporation.

* Corresponding author.

In the pervaporation method, it is desirable for the membranes to be water-selective. Poly(vinyl alcohol) (PVA) is a polymer with high hydrophilicity, excellent membrane formation, and low stability in water. It is predicted that the free amino hydroxyl groups in the chitosan chains and the carbonyl groups in the *N,N*-dimethylacrylamide will increase the stability of the membrane in water, while increasing its hydrophilicity [2,22–24]. Therefore, hydrophilic poly(vinyl alcohol)/(chitosan-*g*-poly(*N,N*-dimethylacrylamide)) (PVA/CS-*g*-PNDMAAm) membranes were used in our study.

In this work, PVA/CS-*g*-PNDMAAm membranes were used for seawater desalination through PV technology. The effects of the pH, CS-*g*-PNDMAAm percentage and, working temperature on the salt rejection and flux were investigated by separating Na/water mixtures with the PV technique. Also, Na removal from Marmara Seawater was performed using the pervaporation technique under optimum conditions.

## 2. Experimental

### 2.1. Materials

Chitosan (CS) (viscosity 200–800 cps, medium molecular weight, deacetylation 75%–85%) and *N,N*-dimethylacrylamide (NDMAAm) (assay 99%) were purchased from Sigma-Aldrich. Poly(vinyl alcohol) (PVA) (average molecular weight value of 89,000–98,000 and a 98%–99% degree of hydrolysis) was supplied by Merck. Ammonium persulfate (APS) and N,N,N,N-tetramethylenediamine (TEMED) were obtained from Aldrich.

### 2.2. Synthesis of CS-g-PNDMAAm graft copolymer

A free radical graft copolymerization technique prepared CS-*g*-PNDMAAm copolymer. For the preparation CS-*g*-PNDMAAm copolymer, CS (2%) was dissolved in 50 mL, 2% (v/v) aqueous acetic acid at room temperature by stirring with a magnetic stirrer. Then the CS solution, which was taken into the 2-necked flask, was taken into the water bath at 60°C. NDMAAm monomer was added and kept in a nitrogen atmosphere for 30 min. Then TEMED and APS were added, and the experiment was continued at 60°C in a nitrogen atmosphere for two more hours. At the end of the experiment, the polymer and homopolymer mixture precipitated in cold acetone was washed in ethanol with the help of a soxhlet, and the homopolymer was removed and the graft copolymer was obtained. The CS-*g*-PNDMAAm copolymer was dried in an oven at 40°C until constant weight. The grafting parameters, including graft yield (GY) and grafting efficiency (GE), were calculated as follows [25]:

$$\mathrm{GY}(\%) = \left(\frac{w_g - w_o}{w_o}\right) \times 100 \tag{1}$$

$$\mathrm{GE}(\%) = \left(\frac{\left(w_g - w_o\right)}{\left(w_g - w_o\right) + w_h}\right) \times 100 \tag{2}$$

where $w_o$, $w_g$, and $w_h$ indicate the weights of the ungrafted chitosan, grafted chitosan, and homopolymer, respectively. In our study, GY was calculated as 35.87% and GE as 17.34%.

### 2.3. Preparation of PVA/CS-g-PNDMAAm membranes

CS-*g*-PNDMAAm membranes were prepared by a solution casting and solvent evaporation technique to be used in the desalination process. 2% PVA solution was prepared by mixing in deionized water at 85°C. 1% CS-*g*-PNDMAAm solution was prepared by mixing in 2% acetic acid at room temperature. CS-*g*-PNDMAAm at concentrations from 0% to 25% were added separately into the PVA solution and mixed until the solutions were homogeneous. The prepared solutions were poured into petri dishes and dried in an oven until completely dry. The thickness of the membranes was measured with a Dasqua brand micrometer, and all membranes were thermally cross-linked at 150°C for 1 h in the oven.

### 2.4. Characterization of the CS-g-PNDMAAm copolymer and the PVA/CS-g-PNDMAAm membrane

Fourier-transform infrared spectroscopy (FTIR) of the CS and CS-*g*-PNDMAAm copolymer was taken using the Agilent Cary 600 Series FTIR spectrometer for the wavelengths between 400 and 4,000 $cm^{-1}$. Thermogravimetric analysis (TGA) of the CS and CS-*g*-PNDMAAm copolymer was conducted by a SETERAM labSys device thermogravimetric analyzer with a temperature range from 0°C to 900°C and heating rate of 10°C/min in $N_2$ atmosphere. The PVA and PVA/CS-*g*-PNDMAAm membranes morphology was observed by scanning electron microscopy–energy-dispersive X-ray analysis (SEM-EDX) (Hitachi SU3500).

### 2.5. Desalination

The desalination pervaporation studies were performed using the apparatus explained in the previous work [26]. The PVA or PVA/CS-*g*-PNDMAAm membranes were attached to the pervaporation cell, put into a water bath with adjustable temperature, and performed the experiments by passing Na/water mixtures through the membrane for 1 h in a vacuum (0.8 mbar). During the pervaporation tests, permeate was collected in traps cooled with liquid nitrogen and weighed, and the Na contents were detected by the flame atomic absorption spectrophotometer (FAAS) (Agilent 240 Duo FAAS) using calibration curves. The optimum operating conditions for Na in FASS were taken to be a wavelength of 589.0 nm, an HCL current of 5.0 mA, an acetylene flow rate of 2.00 L $min^{-1}$, an airflow rate of 13.50 L $min^{-1}$, and a slit width of 0.5 nm. Calibration outcomes were obtained by replicating at least 5 readings. Flux values were decided from the mass of the permeate collected in the traps.

$$J = \frac{Q}{At} \tag{3}$$

$$\mathrm{Rejection}(\%) = \left(\frac{C_F - C_P}{C_F}\right) \times 100 \tag{4}$$

where the mass of permeate is $Q$, the effective membrane area is $A$ (μm), the time is $t$ (min), $C_F$ and $C_P$ represent the Na concentration in the feed and permeate mixture, respectively. All pervaporation experiments in the study were carried out in triplicates, and mean values were calculated for the findings. Besides, the PVA/CS-*g*-PNDMAAm membrane was analyzed by treatment with dilute $HNO_3$ after the experiment to determine the contents of Na retained. The concentration of Na trapped in the membrane was found too low to be detected. This situation indicates that the PVA/CS-*g*-PNDMAAm membrane does not act as an adsorbent in Na removal and it supports that Na does not pass through the membrane due to the pore size of the PVA/CS-*g*-PNDMAAm membrane.

## 3. Results and discussion

### 3.1. Characterizations

The FTIR spectra of CS and CS-*g*-PNDMAAm are shown in Fig. 1. The characteristic peaks of CS and DMAAm are presented in Table 1. The grafting of DMAAm in the IR spectrum of CS-*g*-PNDMAAm is confirmed by characteristics absorption bands at 1,718 and 1,377 $cm^{-1}$ due to C=O and C–N stretching vibration [27].

The TGA curves of the CS and CS-*g*-PNDMAAm copolymer are illustrated in Fig. 2. The degradation in the temperature range of 52.47°C–183.65°C is due to the removal of absorbed water in both CS and CS-*g*-PNDMAAm copolymer structures.

The CS showed noticeable degradation between 210°C and 390°C, with the maximum decomposition rate at about 300°C and weight loss of 61.5%, attributed to the decomposition of the CS main chain. In the TGA curve of CS-*g*-PNDMAAm copolymer, weight loss was observed in three steps in the temperature ranges of 175°C–300°C, 300°C–475°C, and 741°C–900°C. 62.4% weight loss was seen in the second-step with the maximum decomposition temperature about 348°C, which was thought to be exist due to the disruption of C–C and C–N bonds where $CH_4$, $NH_3$, and CO units were separated from the structure. In the third step, with the maximum decomposition temperature of about 813°C, 7.16% weight loss was observed, which is thought to be caused by the disruption of C=O, N–H, and C–H bonds [28].

The SEM-EDX image results of PVA and PVA/CS-*g*-PNDMAAm membranes are shown in Fig. 3. It was observed that the smooth and homogeneous surface of the

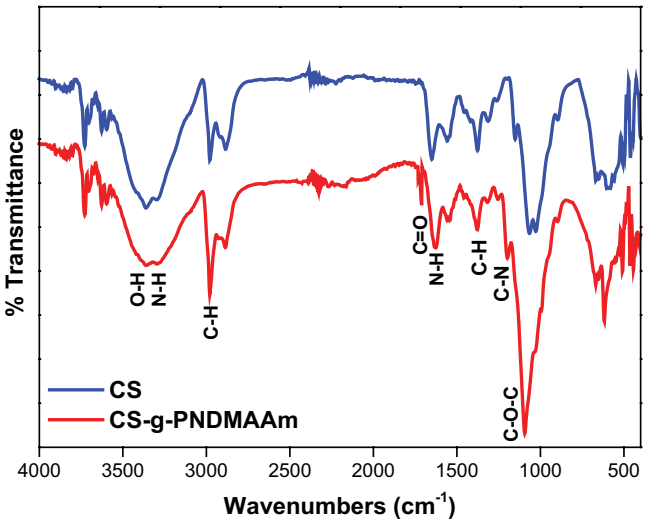


Fig. 1. FTIR spectra of CS and CS-*g*-PNDMAAm.

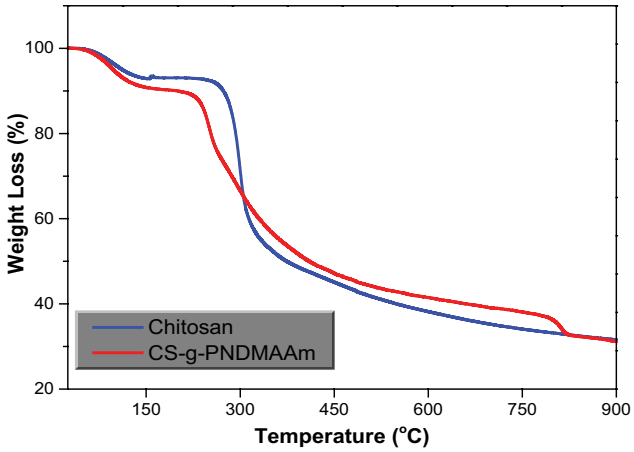


Fig. 2. TGA of CS and CS-*g*-PNDMAAm.

Table 1
Characteristics vibration bands of PVA and PVA-*g*-PNDMAAm membranes

| CS | | CS-*g*-PNDMAAm | |
|---|---|---|---|
| Wavenumber ($cm^{-1}$)/Vibrational band | | Wavenumber ($cm^{-1}$)/Vibrational band | |
| 1,065 | C–O stretching | 1,085 | C–O–C stretching |
| 1,150 | C–N stretching vibrations (amide III) | 1,197 | C–N stretching vibrations (amide III) |
| 1,317 | C–H groups | 1,313 | C–H groups |
| 1,376 | C–H bending vibrations | 1,377 | C–H bending vibrations |
| 1,650 | N–H bending (amide II) | 1,626 | N–H bending (amide II) |
| | | 1,718 | C=O stretching (amide I) |
| 2,884–2,978 | C–H stretching | 2,886–2,979 | C–H stretching |
| 3,362 | OH stretching | 3,361 | OH/NH stretching |

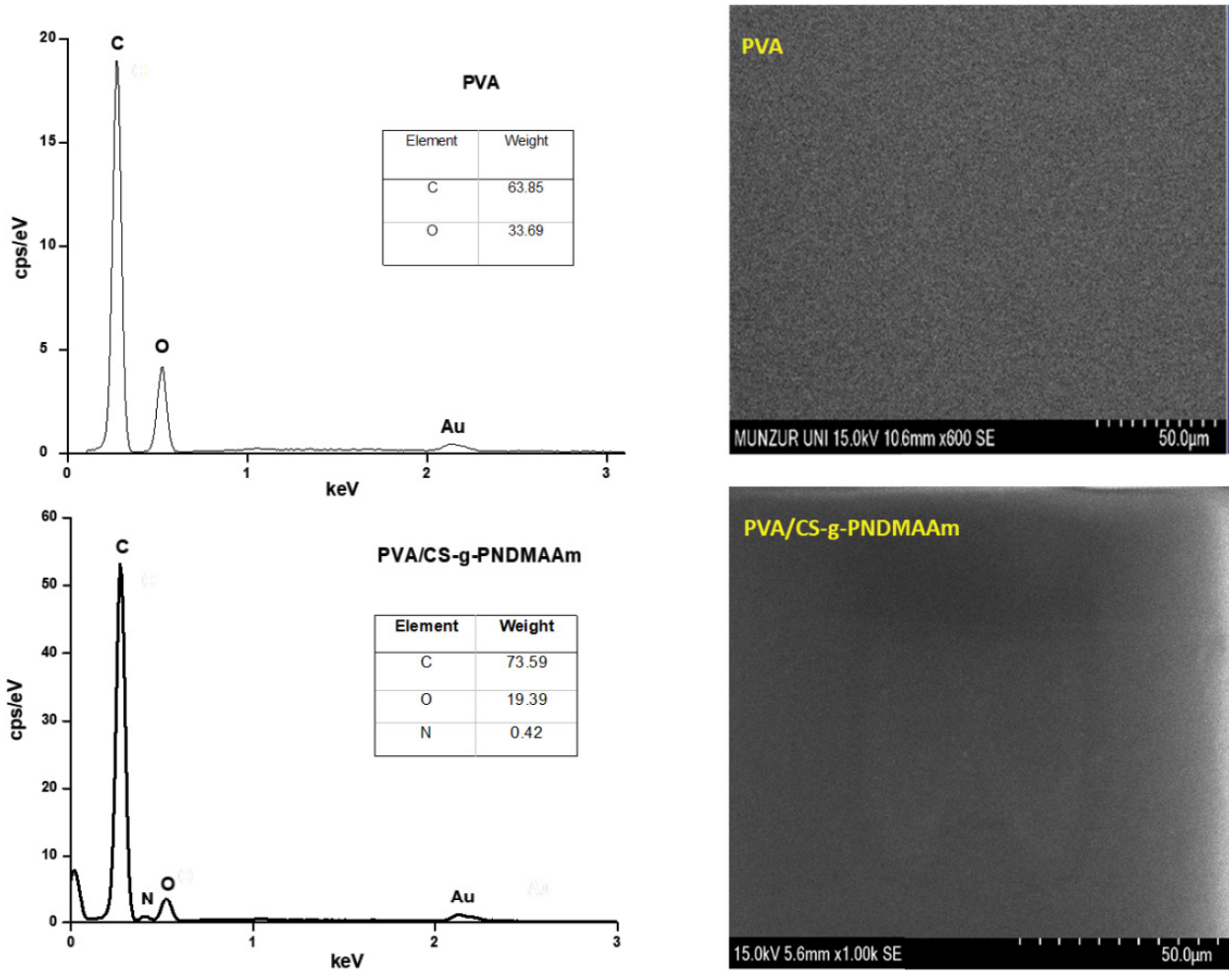


Fig. 3. SEM-EDX image of PVA and PVA/CS-*g*-PNDMAAm membranes.

PVA membrane did not change with the addition of CS-*g*-PNDMAAm copolymer, and the membrane preserved its homogeneous and smooth surface. Investigated the EDX analyses of PVA and PVA/CS-*g*-PNDMAAm membranes, sharp peaks in the range of 0–1 keV disclosed the presence of C and O elements. In the EDX graph, the small peak of N element and the change in the percent values of other elements confirmed that PVA/CS-*g*-PNDMAAm membrane was acquired [29,30].

### 3.2. Pervaporation desalination results

#### 3.2.1. Effect of pH

1,000 ppm synthetic seawater was used to examine the pH effect. When the effect of pH was examined, maximum Na intake was realized at pH 8. The ultimate rejection was found to be 98.6%. The flux value was found to be 204.62 g $m^{-2}$ $h^{-1}$. Since the probability of negative charge on the membrane surface increases in pH 8, it can make it difficult for positively charged ions to pass through. Therefore, the optimum pH value for the $Na^+$ ion was determined as 8 [31].

#### 3.2.2. Effect of CS-g-PNDMAAm percentage

While the effect of CS-*g*-PNDMAAm co-polymer percentage on salt rejection and flux was investigated, 1,000 ppm synthetic seawater was used, and the results are presented in Fig. 5. It was observed that the flux and salt rejection values increased with the increase of the graft co-polymer percentage in the PVA membrane compared to the pristine PVA membrane. As the percentage of CS-*g*-PNDMAAm rose from 0% by weight to 25% by weight, the salt rejection values increased from 96.83% to 99.61%, and the flux values gradually increased from 0.186 to 0.438 kg $m^{-2}$ $h^{-1}$, in 25°C. The increase in flux values can be attributed to the increase in the hydrophilicity of the membrane structure by adding the hydrophilic graft copolymer to the pristine PVA membrane structure. However, the decrease in the crystallinity values obtained from the DSC results also supports the polymer

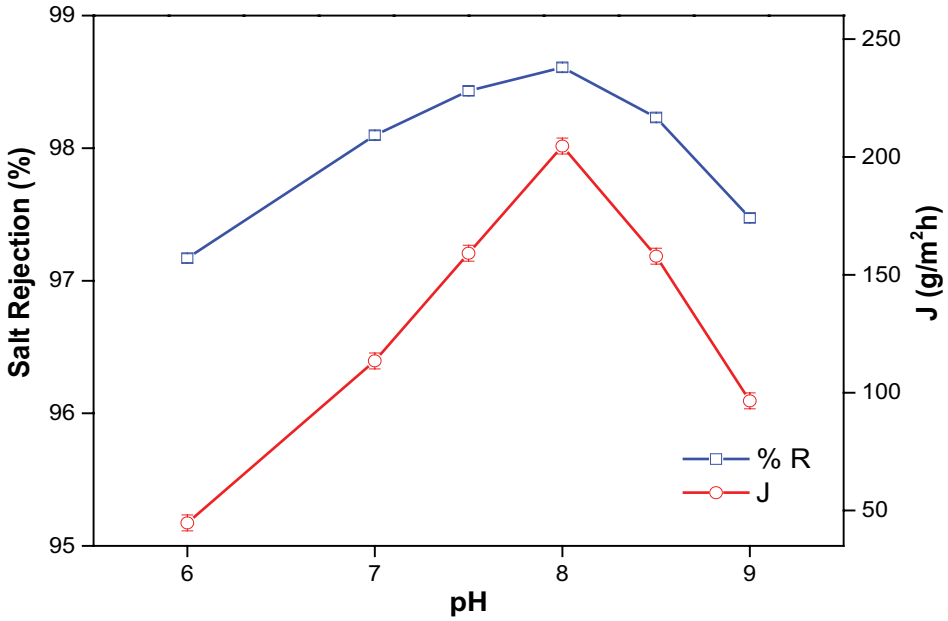


Fig. 4. Effect of pH on salt rejection and flux.

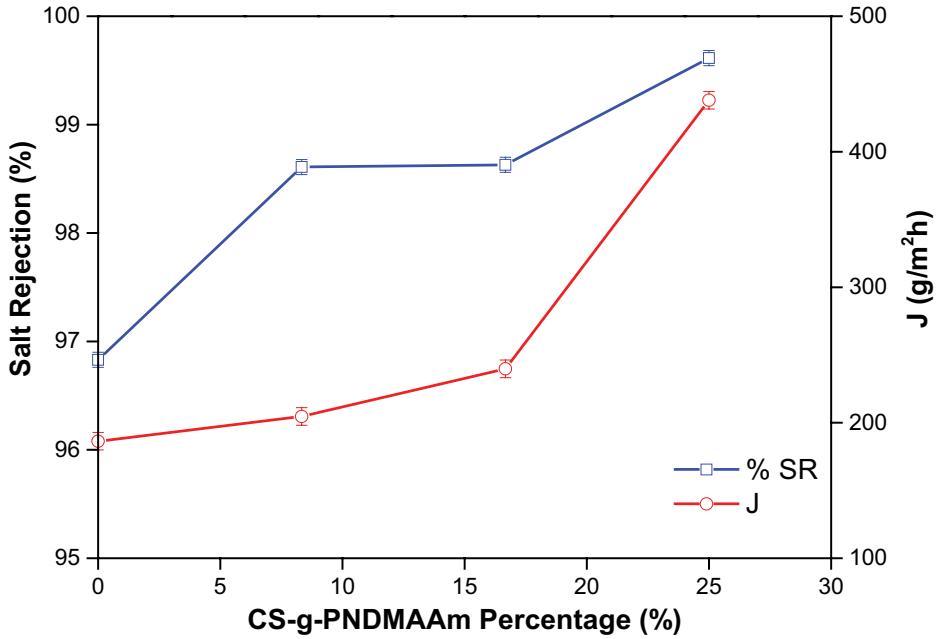


Fig. 5. Effect of CS-*g*-PNDMAAm co-polymer percentage on salt rejection and flux.

chain mobility, increasing the free volume. Thus, with the increase in the hydrophilic character of the membrane, the sorption of water molecules to the membrane will increase, and the diffusion through the membrane and desorption from the membrane water molecules will increase with the increased free volume in the membrane matrix [21,32]. Nigiz [21] synthesized graphene oxide (GO) filled sodium alginate membranes and reported that as the GO content in the membrane structure increased from 0 to 2 wt.%, the flux values gradually increased from 1.63 to 4.89 kg $m^{-2}$ $h^{-1}$.

*3.2.3. Effect of temperature*

It is a known fact that one of the most influential parameters in increasing the flux values in the pervaporation separation process is the temperature increase. The solubilities and diffusions of the molecules that penetrate the membrane in the pervaporation process differ thanks to the vacuum effect that plays a vital role in separation. Since the parameter affecting the solubility is temperature, the number of dissolved molecules will increase with temperature increase. Thus the flux value

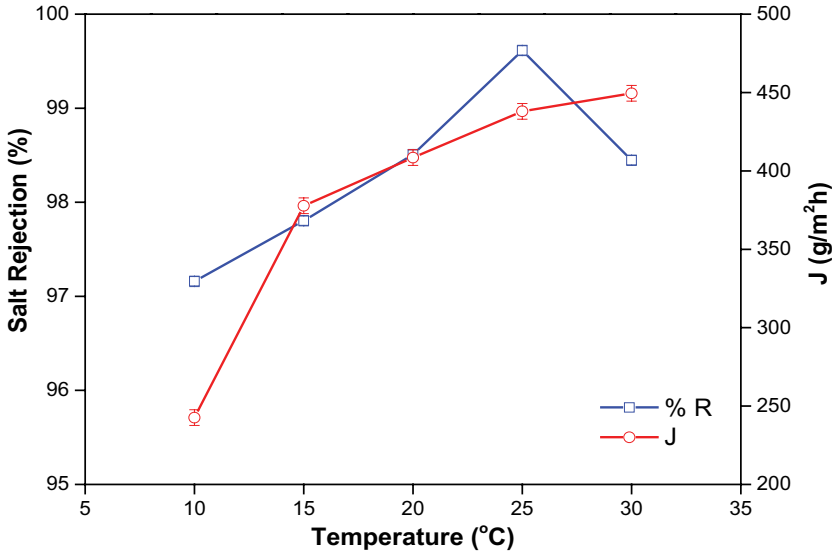


Fig. 6. Effect of temperature on salt rejection and flux.

Table 2
Salt concentrations of the permeate

| CS-*g*-PNDMAAm Percentage | Na concentration in the permeate (ppm) | Temperature (°C) | Na concentration in the permeate (ppm) | pH | Na concentration in the permeate (ppm) |
|---|---|---|---|---|---|
| 0 | 31.7 ± 0.2 | 10 | 28.4 ± 0.1 | 6 | 28.3 ± 0.1 |
| 8.33 | 13.9 ± 0.1 | 15 | 22.0 ± 0.1 | 7 | 19.0 ± 0.1 |
| 16.7 | 13.7 ± 0.1 | 20 | 14.9 ± 0.1 | 7.5 | 15.7 ± 0.1 |
| 25 | 3.86 ± 0.19 | 25 | 3.86 ± 0.08 | 8 | 13.9 ± 0.1 |
| | | 30 | 15.5 ± 0.1 | 8.5 | 17.7 ± 0.1 |
| | | | | 9 | 25.3 ± 0.1 |

will increase as the number of molecules diffused into the membrane increases. In addition, as the rise in temperature increases the polymer chain mobility, it causes an increase in the free volume formed in the polymer matrix and thus an increase in the water absorption capacity of the membrane. Also, as the temperature of the feed solution increases, the vapor pressure on the feed side increases, creating a higher driving force for the separation process [33].

When Fig. 6 is examined, it is seen that the flux values increased from 0.243 to 0.45 kg $m^{-2}$ $h^{-1}$ as the temperature increased from 10°C to 30°C, and the salt rejection values reached their maximum value of 99.6°C at 25°C in the synthetic seawater. Increasing the feed solution to high temperatures in pervaporation desalination processes causes great costs in terms of energy efficiency. Therefore, by achieving high salt rejection at low temperatures in this study, the prices of heating the feed solution to the already economical pervaporation method will also be eliminated [3,34–36].

In the study, the Na concentrations in both the feed solution and the permeate is used in salt rejection calculations (Section 2.5, equality rejection) with the pervaporation method due to the fact that the salt rejection (%) under pH and temperature effect was 98.6 and 99.6, respectively. As the concentrations in the product of the salt rejection results given in Figs. 4–6 are given in Table 2.

### 3.3. Seawater desalination results

The calculated for $Na^+$ ion was found as linearity ($y$ = 0.2222$x$ – 0.0312), correlation coefficient values ($R^2$ = 0.9984), relative standard deviation (RSD) (0.2%–0.6%), limit of detection (LOD) (0.0068 mg $L^{-1}$) and limit of quantification (LOQ) (0.0225 mg $L^{-1}$), which validating the precision of the method. RSDs were found below 1%. Further, the accuracy of the proposed method was also checked by the analysis of certified reference material SRM-NASS-6. In the pervaporation experiments, tests were carried out for seawater samples taken from the Marmara Sea and SRM (NASS-6) seawater samples under optimum conditions obtained using synthetic seawater (Table 3).

NASS-6 trace elements in water obtained from the National Research Council of Canada were used. Recovery tests for analytes in SRM seawater using FAAS are listed in Table 4. The concentrations found by using the presented procedure were in agreement with the certified values.

The physical and chemical properties of Marmara Seawater used in pervaporation studies are presented in Table 5.

The results are presented in Fig. 7. When the results were examined, it was observed that there was an increase in both flux and salt rejection values in Marmara Seawater and SRM seawater samples compared to synthetic seawater. This situation can be attributed to the decrease in ion transmission through the membrane and increased water transmission due to the presence of ions other than sodium and chlorine in seawater and the repulsion forces between these ions [37,38].

Table 3
Chemical properties of synthetic seawater

| Ions (added as) | Concentration (mg $L^{-1}$) |
|---|---|
| $K^+$, $Cl^-$ (KCl) | 600 |
| $Ca^{2+}$ ($CaCl_2$) | 400 |
| $Cu^{2+}$ ($Cu(NO_3)_2 \cdot 3H_2O$) | 5 |
| $Fe^{3+}$ ($Fe(NO_3)_3 \cdot 9H_2O$) | 1 |
| $Zn^{2+}$ ($Zn(NO_3)_2$) | 1 |
| $Na^+$, $Cl^-$ (NaCl) | 1,000 |

## 4. Conclusions

This study used PVA/CS-*g*-PNDMAAm membranes for seawater desalination through pervaporation technology. CS-*g*-PNDMAAm copolymers were synthesized and characterized by FTIR and TGA. SEM-EDX characterized the surfaces of PVA/CS-*g*-PNDMAAm membranes. In the separation of Na/water mixtures by PV technique, 25% CS, room temperature, and basic medium (pH 8)

Table 5
Physical and chemical properties of Marmara Seawater

| | Marmara Seawater |
|---|---|
| pH | 8.3 |
| Na (mg $L^{-1}$) | 2,499 ± 13 |
| Ca (mg $L^{-1}$) | 212 ± 2 |
| K (mg $L^{-1}$) | 280 ± 11 |
| Fe (mg $L^{-1}$) | 0.076 ± 0.009 |
| Zn (mg $L^{-1}$) | 0.056 ± 0.009 |
| Cu (mg $L^{-1}$) | 0.017 ± 0.009 |

Table 4
Recovery tests for analytes in SRM seawater (NASS-6) by using FAAS

| | Added (mg $L^{-1}$) | Found (mg $L^{-1}$) | Recovery (%) |
|---|---|---|---|
| Na (mg $L^{-1}$) | – | 2,169 ± 12 | – |
| | 1,000 | 3,172 ± 15 | 100 ± 1 |
| Ca (mg $L^{-1}$) | – | 104 ± 2 | – |
| | 50 | 156 ± 1 | 102 ± 1 |
| K (mg $L^{-1}$) | – | 124 ± 1 | – |
| | 50 | 175 ± 1 | 101 ± 1 |
| Fe (μg $L^{-1}$) | Certified value/0.495 ± 0.046 | 0.489 ± 0.022 | 98.8 ± 3.2 |
| Zn (μg $L^{-1}$) | Certified value/0.257 ± 0.020 | 0.265 ± 0.013 | 103 ± 6 |
| Cu (μg $L^{-1}$) | Certified value/0.248 ± 0.025 | 0.242 ± 0.017 | 97.6 ± 2.2 |

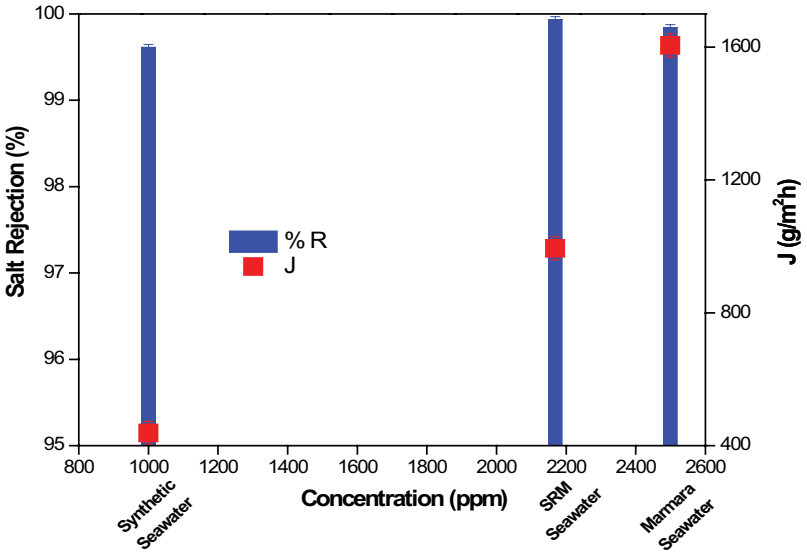


Fig. 7. Compared with synthetic seawater of Marmara Seawater and SRM seawater samples.

separation was found to be optimum. In removing Na from Marmara Seawater using the pervaporation technique, the maximum salt rejection was found to be 99.94, while the flux was 993.52 g $m^{-2}$ $h^{-1}$ under optimum conditions. According to WHO, daily salt intake ranges from 2.07 to 4.77 g $d^{-1}$ [39].When this situation is evaluated with our experimental studies, it shows that the Na content of the water obtained at the end of the pervaporation experiments will not exceed the daily intake value.

The excellent hydrophilic nature of PVA/CS-*g*-PNDMAAm membranes could be attributed to the stability of the CS-*g*-PNDMAAm structural link. As a result, PVA/CS-*g*-PNDMAAm membranes show potential in desalination by pervaporation.

## Data availability

All data are incorporated in the manuscript. No additional data are available for sharing.

## Declaration of competing interest

The authors declare no conflict of interest.

## References


[1] Q. Wang, N. Li, B. Bolto, M. Hoang, Z. Xie, Desalination by pervaporation: a review, Desalination, 387 (2016) 46–60.

[2] X. Qian, N. Li, Q. Wang, S. Ji, Chitosan/graphene oxide mixed matrix membrane with enhanced water permeability for high-salinity water desalination by pervaporation, Desalination, 438 (2018) 83–96.

[3] B. Liang, K. Pan, L. Li, E.P. Giannelis, B. Cao, High performance hydrophilic pervaporation composite membranes for water desalination, Desalination, 347 (2014) 199–206.

[4] I. Prihatiningtyas, B. Van der Bruggen, Nanocomposite pervaporation membrane for desalination, Chem. Eng. Res. Des., 164 (2020) 147–161.

[5] L.F. Greenlee, D.F. Lawler, B.D. Freeman, B. Marrot, P. Moulin, Reverse osmosis desalination: water sources, technology, and today's challenges, Water Res., 43 (2009) 2317–2348.

[6] M. Qasim, M. Badrelzaman, N.N. Darwish, N.A. Darwish, N. Hilal, Reverse osmosis desalination: a state-of-the-art review, Desalination, 459 (2019) 59–104.

[7] W. Falath, Novel stand-alone PVA mixed matrix membranes conjugated with graphene oxide for highly improved reverse osmosis performance, Arabian J. Chem., 14 (2021) 103109, doi: 10.1016/j.arabjc.2021.103109.

[8] M. Liu, Q. He, Z. Guo, K. Zhang, S. Yu, C. Gao, Composite reverse osmosis membrane with a selective separation layer of double-layer structure for enhanced desalination, anti-fouling and durability properties, Desalination, 499 (2021) 114838, doi: 10.1016/j.desal.2020.114838.

[9] D.M. Warsinger, J. Swaminathan, E. Guillen-Burrieza, H.A. Arafat, J.H. Lienhard V, Scaling and fouling in membrane distillation for desalination applications: a review, Desalination, 356 (2015) 294–313.

[10] B. Li, K.K. Sirkar, Novel membrane and device for vacuum membrane distillation-based desalination process, J. Membr. Sci., 257 (2005) 60–75.

[11] W.J. Lee, Z.C. Ng, S.K. Hubadillah, P.S. Goh, W.J. Lau, M.H.D. Othman, A.F. Ismail, N. Hilal, Fouling mitigation in forward osmosis and membrane distillation for desalination, Desalination, 480 (2020) 114338, doi: 10.1016/j.desal.2020.114338.

[12] J. Ravi, M.H.D. Othman, T. Matsuura, M. Ro'il Bilad, T.H. El-Badawy, F. Aziz, A.F. Ismail, M.A. Rahman, J. Jaafar, Polymeric membranes for desalination using membrane distillation: a review, Desalination, 490 (2020) 114530, doi: 10.1016/j.desal.2020.114530.

[13] R. Castro-Muñoz, Breakthroughs on tailoring pervaporation membranes for water desalination: a review, Water Res., 187 (2020) 116428, doi: 10.1016/j.watres.2020.116428.

[14] H. Zeng, S. Liu, J. Wang, Y. Li, L. Zhu, M. Xu, C. Wang, Hydrophilic SPEEK/PES composite membrane for pervaporation desalination, Sep. Purif. Technol., 250 (2020) 117265, doi: 10.1016/j.seppur.2020.117265.

[15] C. Zhou, J. Zhou, A. Huang, Seeding-free synthesis of zeolite FAU membrane for seawater desalination by pervaporation, Microporous Mesoporous Mater., 234 (2016) 377–383.

[16] Y.L. Xue, J. Huang, C.H. Lau, B. Cao, P. Li, Tailoring the molecular structure of crosslinked polymers for pervaporation desalination, Nat. Commun., 11 (2020), doi: 10.1038/s41467-020-15038-w.

[17] E. Halakoo, X. Feng, Layer-by-layer assembly of polyethyleneimine/graphene oxide membranes for desalination of high-salinity water via pervaporation, Sep. Purif. Technol., 234 (2020) 116077, doi: 10.1016/j.seppur.2019.116077.

[18] C.H. Cho, K.Y. Oh, S.K. Kim, J.G. Yeo, P. Sharma, Pervaporative seawater desalination using NaA zeolite membrane: mechanisms of high water flux and high salt rejection, J. Membr. Sci., 371 (2011) 226–238.

[19] Z. Xie, M. Hoang, T. Duong, D. Ng, B. Dao, S. Gray, Sol–gel derived poly(vinyl alcohol)/maleic acid/silica hybrid membrane for desalination by pervaporation, J. Membr. Sci., 383 (2011) 96–103.

[20] L. Gazagnes, S. Cerneaux, M. Persin, E. Prouzet, A. Larbot, Desalination of sodium chloride solutions and seawater with hydrophobic ceramic membranes, Desalination, 217 (2007) 260–266.

[21] F. Ugur Nigiz, Graphene oxide-sodium alginate membrane for seawater desalination through pervaporation, Desalination, 485 (2020) 114465, doi: 10.1016/j.desal.2020.114465.

[22] C. Fang, Y. Jing, Y. Zong, Z. Lin, Effect of *N,N*-dimethylacrylamide (DMA) on the comprehensive properties of acrylic latex pressure sensitive adhesives, Int. J. Adhes. Adhes., 71 (2016) 105–111.

[23] D.K. Mishra, J. Tripathy, K. Behari, Synthesis of graft copolymer (k-carrageenan-*g*-*N,N*-dimethylacrylamide) and studies of metal ion uptake, swelling capacity and flocculation properties, Carbohydr. Polym., 71 (2008) 524–534.

[24] Y.A. Maher, M.E.A. Ali, H.E. Salama, M.W. Sabaa, Preparation, characterization and evaluation of chitosan biguanidine hydrochloride as a novel antiscalant during membrane desalination process, Arabian J. Chem., 13 (2020) 2964–2981.

[25] N. Isiklan, F. Kursun, M. Inal, Graft copolymerization of itaconic acid onto sodium alginate using ceric ammonium nitrate as initiator, J. Appl. Polym. Sci., 114 (2009) 40–48.

[26] F. Kurşun, Application of PVA-b-NaY zeolite mixture membranes in pervaporation method, J. Mol. Struct., 1201 (2020) 127170, doi: 10.1016/j.molstruc.2019.127170.

[27] J. Tripathy, D.K. Mishra, M. Yadav, K. Behari, Synthesis, characterization and applications of graft copolymer (Chitosan-*g*-*N,N*-dimethylacrylamide), Carbohydr. Polym., 79 (2010) 40–46.

[28] G. Ma, D. Yang, Q. Li, K. Wang, B. Chen, J.F. Kennedy, J. Nie, Injectable hydrogels based on chitosan derivative/polyethylene glycol dimethacrylate/*N,N*-dimethylacrylamide as bone tissue engineering matrix, Carbohydr. Polym., 79 (2010) 620–627.

[29] M. Mende, D. Schwarz, C. Steinbach, R. Boldt, S. Schwarz, Simultaneous adsorption of heavy metal ions and anions from aqueous solutions on chitosan—investigated by spectrophotometry and SEM-EDX analysis, Colloids Surf., A, 510 (2016) 275–282.

[30] R. Karthik, S. Meenakshi, Removal of Pb(II) and Cd(II) ions from aqueous solution using polyaniline grafted chitosan, Chem. Eng. J., 263 (2015) 168–177.

[31] P. Zhao, Y. Xue, R. Zhang, B. Cao, P. Li, Fabrication of pervaporation desalination membranes with excellent chemical resistance for chemical washing, J. Membr. Sci., 611 (2020) 118367, doi: 10.1016/j.memsci.2020.118367.

[32] R. Zhang, B. Liang, T. Qu, B. Cao, P. Li, High-performance sulfosuccinic acid cross-linked PVA composite pervaporation membrane for desalination, Environ. Technol. (United Kingdom), 40 (2019) 312–320.

[33] S.G. Chaudhri, J.C. Chaudhari, P.S. Singh, Fabrication of efficient pervaporation desalination membrane by reinforcement of poly(vinyl alcohol)-silica film on porous polysulfone hollow fiber, J. Appl. Polym. Sci., 135 (2018) 1–13.
[34] Y. Wang, H. Rong, L. Sun, P. Zhang, Y. Yang, L. Jiang, S. Wu, G. Zhu, X. Zou, Fabrication and evaluation of effective zeolite membranes for water desalination, Desalination, 504 (2021) 114974, doi: 10.1016/j.desal.2021.114974.
[35] P.S. Singh, S.G. Chaudhri, A.M. Kansara, W. Schwieger, T. Selvam, S. Reuss, V.K. Aswal, Cetyltrimethylammonium bromide-silica membrane for seawater desalination through pervaporation, Bull. Mater. Sci., 38 (2015) 565–572.
[36] V.G. Gude, N. Nirmalakhandan, S. Deng, A. Maganti, Feasibility study of a new two-stage low temperature desalination process, Energy Convers. Manage., 56 (2012) 192–198.
[37] J. Safaei, P. Xiong, G. Wang, Progress and prospects of two-dimensional materials for membrane- based water desalination, Mater. Today Adv., 8 (2020) 100108, doi: 10.1016/j.mtadv.2020.100108.
[38] J. Imbrogno, G. Belfort, Membrane desalination: where are we, and what can we learn from fundamentals?, Annu. Rev. Chem. Biomol. Eng., 7 (2016) 29–64.
[39] Guideline: Sodium Intake for Adults and Children, World Health Organization, Geneva, 2012. Available at: https://www.ncbi.nlm.nih.gov/books/NBK133309/